FLOATECH

D5.2. Report on the LCOE improvement of AWM controlled floating wind farms

DATE OF DELIVERY - 31/10/2023

AUTHORS - D. P. COIRO, G. TROISE, G. LAZZERINI, A. GRIECO, F. PAPI, A. BIANCHINI, D. VAN DEN BERG

SEAPOWER SCRL, UNIVERSITY OF FLORENCE, TECHNISCHE UNIVERSITÄT BERLIN, SAIPEM S.A., IDEOL S.A.

This project has received funding from the European Union's Horizon 2020 research and innovation programme under grant agreement No 101007142

FLOATECH
THE FUTURE OF FLOATING WIND TURBINES

Document track details

Project acronym	FLOATECH
Project title	Optimization of floating wind turbines using innovative control techniques and fully coupled open-source engineering tool
Starting date	01.01.2021
Duration	36 months
Programme	H2020-EU.3.3.2. - Low-cost, low-carbon energy supply
Call identifier	H2020-LC-SC3-2020-RES-RIA
Grant Agreement No	101007142

Deliverable Information	
Deliverable number	5.2
Work package number	5
Deliverable title	Report on the LCOE improvement of AWM controlled floating wind farms
Lead beneficiary	SEAPOWER
Author	D.P. Coiro, G. Troise, G. Lazzerini, A. Grieco, F. Papi, A. Bianchini, Daniel van den Berg
Reviewers	J.W. van Wingerden, A. R. M. Hegazy (TUDelft) Marie-Laure Ducasse (Saipem)
Due date	31/10/2023
Actual submission date	30/10/2023
Type of deliverable	Report
Dissemination level	Public

Version management

Document history and validation			
Version	**Name**	**Date**	**Comment**
V 1	D.P. Coiro, G. Troise, A. Grieco, G. Lazzerini, F. Papi, A. Bianchini, Daniel van den Berg	09/10/2023	First version
V 2	Revision by TU Delft and Saipem		

Background: about the FLOATECH project

The FLOATECH project is a Research and Innovation Action funded by the European Union's H2020 programme aiming to increase the technical maturity and the cost competitiveness of floating offshore wind (FOW) energy. This is particularly important because, due to the limitations of available installation sites onshore, offshore wind is becoming crucial to ensure the further growth of the wind energy sector.

The project is implemented by a European consortium of 5 public research institutions with relevant skills in the field of offshore floating wind energy and 3 industrial partners, two of which have been involved in the most recent developments of floating wind systems.

The approach of FLOATECH can be broken down into three actions:

- The development, implementation and validation of a user-friendly and efficient design engineering tool (named QBlade-Ocean) performing simulations of floating offshore wind turbines with an unprecedented combination of aerodynamic and hydrodynamic fidelity. The advanced modelling theories will lead to a reduction of the uncertainties in the design process and an increase of turbine efficiency.
- The development of two innovative control techniques: the Active Wave-based feed-forward Control, combining wave prediction and anticipation of induced platform motion to reduce oscillations and loads, and the Active Wake Mixing, aimed at minimizing wake effects in floating wind farms, leading to a net increase in the annual energy production of the farm.
- The economic analysis of these concepts to demonstrate qualitatively and quantitatively the impact of the developed technologies on the Levelized Cost of Energy (LCOE) of FOW technology.

In addition to the technological and economic impacts, the project is expected to have several impacts at societal, environmental and political levels, such as: public acceptance, due to noise and visibility issues of FOWT; very low impact on biodiversity and wildlife habitat since no foundations are needed be to installed into the seabed; the use of less material and space thanks to an environment friendly design; the promotion of the installation of FOW in transitional water depths (30-50 m and larger), as the costs for FOW at those locations can become more competitive compared to the fixed bottom foundations, although some efforts are still needed to solve the complex technical problems related to the mooring and floater design, particularly for large size wind turbines.

Table of contents

List of acronyms and abbreviations

Acronym / Abbreviation	Meaning / Full text
FOW	Floating Offshore Wind
FOWT	Floating Offshore Wind Turbine
LCOE	Levelized Cost of Energy
CRF	Capital Recovery Factor
AEP	Annual Energy Production
WP	Work package
AWC	Active Wave Control
AWM	Active Wake Mixing
FF	Feed-forward
DEL	Damage Equivalent Load
GDP	Gross Domestic Product
PPI	Producer Price Index (TPPI indicates the total PPI, comprising domestic and international trading price index)

List of symbols

Acronym / Abbreviation	Meaning / Full text
CAPEX	Capital Expenditures
OPEX	Operational Expenditures
DECEX	Decommissioning costs
$M_{xy_{TB}}$	Combined bending moment at the tower base

1 EXECUTIVE SUMMARY

This document reports a part of the results of Work Package (WP) 5 of the Floatech project. The main goal of WP 5 is the estimation of the impact of the newly developed control technologies on FOWT economic performance. Specifically, WP 5 will investigate the effects on the overall component costs due to the introduction of two new control strategies: Active Wave Control (AWC), related to the feed-froward control methodology developed in WP 3 of Floatech project, and Active Wake Mixing (AWM), related to the wake mixing control strategy developed in WP 4. Two different tasks are dedicated to the analysis of the new control strategies: Task 5.1, dedicated to the study of AWC, and Task 5.2 dedicated to AWM. In order to investigate the economic effects of the implementation of the new controls, a cost model, parametrized on the main geometrical and performance data of the FOWT, is simultaneously under development in Task 5.3. This report is specifically related to the economic assessment of the AWM control strategy. The current study exploits the results of a set of simulations performed using QBlade in order to estimate the loads on the main FOWT components and the effect of the control on power production performance. The methodology used to estimate the possible improvements due to the newly introduced control technology is based on a hybrid approach: on one hand, some cost contributions will be estimated using expressions based on statistical regression, typically derived from literature, while, on the other hand, the costs of the FOWT components mainly affected by the control variation will be estimated using a simplified preliminary design calculations, in order to evaluate possible changes in design parameters due to the predicted load variations.

In the process of LCOE estimation, possible changes in the Annual Energy Production (AEP) need also to be accounted for. The results of the study are presented in terms of variation of the LCOE between a reference case and a modified design including the AWM control technology, using the control strategy designated as Helix, developed by TU Delft. Based on the results of the currently implemented cost model, a reduction of the LCOE in a range between about -1% and -6%, depending on wind farm size, is expected using the newly implemented control strategy for a given wind climate and a simplified square farm layout.

2 INTRODUCTION

Wind energy has already reached a high level of technological maturity in onshore applications, offering reliable and affordable technical solutions, which would be very attractive for potential renewable energy stakeholders. On the contrary, offshore applications still present some technical issues limiting the diffusion of such technology, particularly in the case of floating offshore plants. Both the limitations of available onshore suitable sites and the large amount of wind energy resource potentially available in offshore locations push towards an increase in the exploitation of marine areas for wind energy production, also driven by EU and national polices, prospecting global targets for the total installed power from renewable sources. A total of 30 GW is currently installed offshore in Europe by the end of 2022, according to [1], and an increase in installed power is predicted for the next 5 years, although, due to the conjunctural economic conditions with high inflation rate and material prices, the predicted installation rate is currently lower than the expected theoretical trend required to meet the installed power target.

Among the operating offshore plants, the vast majority currently comprises installations with fixed bottom foundations. The costs of bottom fixed offshore wind turbine rapidly increase with the depth of the installation site [2], thus limiting the exploitation of the potentially more attractive areas located far from the coastline, with expectedly higher wind resource and with lower visual impact. On the other hand, Floating Offshore Wind Turbines (FOWT) allows to overcome the limitations intrinsic to bottom-fixed installations, but also pose several challenging technological issues. The *Floatech* project was mainly focused on the development of a simulation tool (QBlade-Ocean) aimed at simulating the behaviour of floating wind turbines, accurately and efficiently, under a wide range of environmental conditions. Concurrently two new technologies were introduced during the Floatech project with the objective of improving FOWT behaviour using advanced control strategies. In the AWC control technique a feed-forward strategy, based on the observation of the incoming wave field through a radar sensor, is used to improve the desired response of a FOWT by acting on its pitch control system, as described in deliverable 3.1 [3]. The AWM control technique, on which this work is mainly focused, is intended to improve the wake velocity recovery downstream of the turbine on which the control is implemented, thereby reducing the effect of wake interaction and the related energy production loss in a wind farm. Wake recovery enhancement is obtained by promoting the wake mixing with the surrounding flow inducing an oscillating motion of the wake. Different possible wake mixing procedures can be defined. This study is focused on the case indicated as “Helix”, in which wake oscillations are generated through a cyclic variation of the individual blade pitch. The overall working principle, on which this control strategy relies, is presented in [4]. During Floatech WP 4, moreover, a further possibility of improvement of the wake mixing action has been investigated. For the case of floating wind turbines, the possibility of increasing the oscillatory motion of the wake by augmenting the yaw response of the platform has been explored: an optimization procedure has been defined in order to match the platform yaw response characteristics with the requirements of the Helix control strategy, with the objective of augmenting wake oscillations at the required excitation frequency of the control.

The purpose of the study presented in this document is to provide an estimate of the effect of the AWM control technique on the overall costs and energy production of a FOWT, which is summarized using the

Levelized Cost Of Energy (LCOE), a technoeconomic parameter commonly used for economic assessment of energy production plant.

3 GENERAL DEFINTIONS AND ASSUMPTIONS

The Levelized Cost of Energy (LCOE) will be assumed in this study as the principal indicator for the technoeconomic assessment of a FOWT installation, defined using the following expression:

$$LCOE = \frac{CAPEX \times CRF + OPEX + DECEX \times \frac{i}{(1+i)^t - 1}}{AEP} \tag{1}$$

In the above relation $CAPEX$, measured in €, indicates the capital expenditures, $OPEX$ represents the annual operating costs, measured in €/year, $DECEX$, in €, is referred to the decommissioning costs, AEP is the annual energy production, measured in MWh/year, t is the total duration of the project and the factor i is a *discount rate* assumed to estimate the present value of future costs and energy production at the start time of the project, which also affects the *Capital Recovery Factor* (CRF) estimated as

$$CRF = \frac{i(1+i)^t}{(1+i)^t - 1} \tag{2}$$

The definitions and assumptions reported in this section have already been introduced in deliverable D5.1 [5], with some more details, and are briefly recalled here for completeness. The total time of the project, t, is considered equal to 20 years.

A value equal to 11.5% has been assumed for the discount rate, based on the value of Weighted Averaged Capital Cost (WACC), based on literature data [6] and accounting for inflation effects at the reference year 2022. Some details on the estimation of the discount rate are also reported in deliverable D5.1 [5].

4 FLOATING TURBINE CONFIGURATION AND CONTROL

For the present study a specific choice of the analysed configuration has been made. Specifically, the Softwind configuration (described in [7]) has been considered, a design solution developed at Ecole Central de Nantes (ECN) and subjected to an intensive experimental test campaign, and already used for the analyses performed in Floatech WP2. The following assumptions on system modelling has been done:

- rotor and nacelle from DTU 10MW RWT [8] have been considered;
- the tower from OOStar project [9] [10] has been considered, consistently with the assumptions of WP2;
- the Softwind platform studied at ECN has been considered (with a modification of the mooring line system described in 5.2.1).

The geometry of the overall system is illustrated in the following figure.

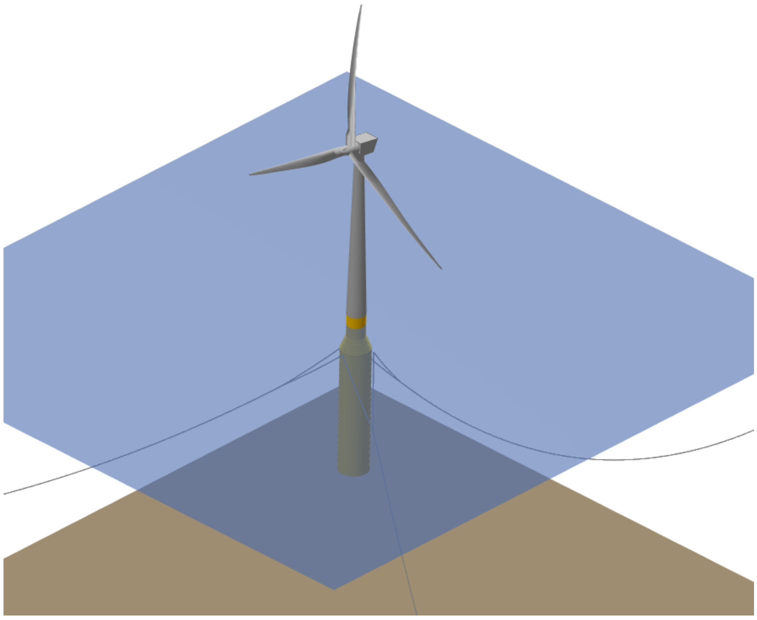

Figure 1. Softwind model.

The platform has a spar buoy configuration with a mooring system composed by a set of three mooring lines connected to the platform by a system of delta connected bridles.

The rotor geometry is descripted in more details in [11]. Two control systems will be considered in the analysis: the baseline control will be the original standard control, already used in WP5 simulations for the AWC baseline related study, which implements a standard blade pitch control for power limitation, while the modified control will implement the AWM control technique in the so-called Helix solution. As previously mentioned, this control strategy, described for example in [4], uses an individual blade pitch control to generate an oscillation of the wake, which, in turn, may reduce wake losses on the trailing turbines. The improvement of the wake recovery mechanism can be further enhanced in the case of floating turbines by promoting the yaw oscillating motion of the platform. For a FOWT, the yawing moment, generated by the cyclic pitch control action, can induce a yaw forced oscillation, which may, in turn, increase the wake oscillation, magnifying the expected wake recovery. As previously said, a modified configuration of the platform has been searched for, with the aim to optimize the effect of the platform oscillation. The mooring configuration has shown in the analysis a large impact on yaw response for a relatively small modification of the design variables. Thus, for the analysis of the expected performance improvement with the Helix control, a modified platform configuration will be used with a modified mooring system, as described in more detail in 5.2.1.

5 METHODOLOGY

5.1 GENERAL APPROACH FOR THE DEFINITION OF POSSIBLE DESIGN VARIATIONS

The methodology used for the evaluation of the effects of load and performance variation due to the control strategy is shared with the work reported in Floatech deliverable D5.1 [5]. The effect of changing the control strategy can be observed in two different aspects of FOWT response: on one hand, varied loads can influence structure sizing, requiring stiffening and strengthening of components, or allowing for structural mass reduction, depending on the sense of load variation; on the other hand, the power production performance can also be affected by the modification of control strategy. Both these effects can influence the final value of the LCOE, the variation of loadings affecting the component costs and the performance variation influencing the annual energy production (AEP). In this study, several components, deemed primarily affected by the variation of the control, has been identified. For these components, a design modification procedure has been defined. Starting from an initial configuration, the main characteristic dimensions of the considered components have been modified, with the purpose to preserve the same structural safety level of the original configuration.

The components for which this procedure is applied are indicated in the following list:

- the rotor blade;
- the tower;
- the platform;
- the mooring lines.

More details on the design revision procedure are reported in [5]. Other components not included in the previous list have been considered as well in the overall cost assessment, using cost estimation laws typically based on regression relations, available in literature [12] [13] [14].

5.2 MOORING COSTS

The effect of mooring on the overall cost of the floating wind turbine is described separately with some further detail. In fact, prior to the simulation analysis of the FOWT response with the innovative control system, a preliminary optimization study was performed in order to search for a suitable configuration in compliance with the operation of the AWM control, using the Helix strategy.

5.2.1 Mooring system design revision

As already noted, for the specific case of the AWM control, an optimization has been performed in order enhance the response of the platform in compliance with the AWM control technique. Specifically, an optimization procedure was implemented in order to search for the maximum yaw amplitude under a given yawing moment, simulating the moment applied on the platform by the Helix control strategy, through the cyclic change of the individual blade pitch. This periodic pitch variation can be arranged in such a way to generate an equivalent sinusoidal yawing moment by governing the variation of individual blade loads during a rotor revolution. The oscillation of the wake behind the turbine has shown to be potentially beneficial for the reduction of wake losses in a farm, increasing the incoming wind speed level on the trailing turbines in a series of turbine rows. Such improvement in wake velocity recovery may be explained partly considering the increased wake mixing induced by the destabilization of the wake due the forced yawing oscillations; moreover, an additional beneficial effect can be related to the wake deflection which tends to steer the wake away from the trailing turbine, thereby reducing the velocity reduction experienced by the downstream turbine (more details may be found in [15]). In the case of floating wind farms, the motion of the platform can be exploited to further increase this potential improvement; in the present study, prior to the simulations for the determination of wake recovery

behaviour, a dedicated study has been performed in order to optimize the mooring line system with the objective to increase the yaw oscillation response. Aiming at this purpose, the optimization framework developed in Floatech WP4 has been used. Thus, starting from the Softwind original mooring configuration, a modified mooring line arrangement has been defined and considered in the simulations for further analyses. A first kind of variation is related to the choice of the type of mooring line system. The Softwind model uses a bridled configuration: three connection points are placed on the platform and from each connection point two bridles start; the bridles coming from two adjacent fairleads are joined together, in a delta connection, to a single line which is finally linked to the seabed anchor. This system has been simplified, considering a simple three-line mooring system arrangement. This choice is mainly due to the opportunity to reduce the stiffness of the mooring system in order to increase the yaw response to the Helix control exciting moment. The simple three-line system has shown, in fact, a lower yaw stiffness, which is desirable in the perspective of enhancing the yaw response amplitude.
The optimization process starts from the initial configuration with given mooring line length and fairlead positions, then it iteratively searches for a mooring configuration with varied lengths and attachment points with the objective to increase the yaw oscillation amplitude. A simulation-based approach is used: a series of simulations are run, without waves, at the rated wind speed condition, while an external yaw moment is applied to simulate the action of the Helix control action. The design variable space (defined by the mooring cable length and the fairlead radial and vertical positions) is explored using a differential evolution algorithm, searching for the maximum yaw response amplitude. The variables considered in the optimization process (mooring length, fairlead radius and fairlead height) are illustrated in the following figure:

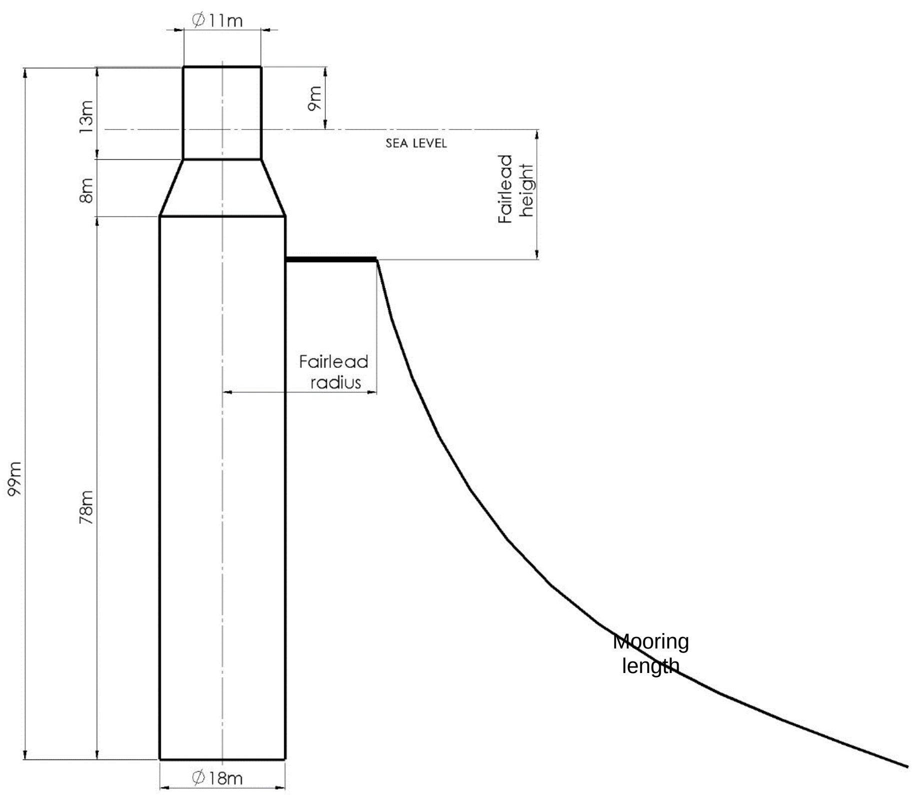

Figure 2. Variables considered in the mooring preliminary optimization procedure aimed at matching Helix control requirements.

A simplified model has been considered, similar to the one developed during task 4.1 of WP4: the effect of the Helix control has been, in fact, simulated using a given external yaw moment applied at the tower top, with a sinusoidal time history of given amplitude and frequency; the characteristics of such forcing yaw moment (100 s period and 10.1 MNm amplitude) were determined from previous studies carried out by the TU Delft team, during the activities for Floatech WP4.

As stated before, after the design revision aimed at matching the AWM control requirements, a new mooring line configuration is considered for further analyses. Figure 3 shows the modified mooring line arrangement. Moreover, the characteristics of the modified mooring system (indicated as "*modified Softwind case"*), compared to the original data (indicated as "*original Softwind case*"), are reported in Table 1. It can be noted that the length of the mooring line is slightly smaller and that the position of fairlead has been slightly raised towards sea water level and shifted outwards with respect to the original configuration.

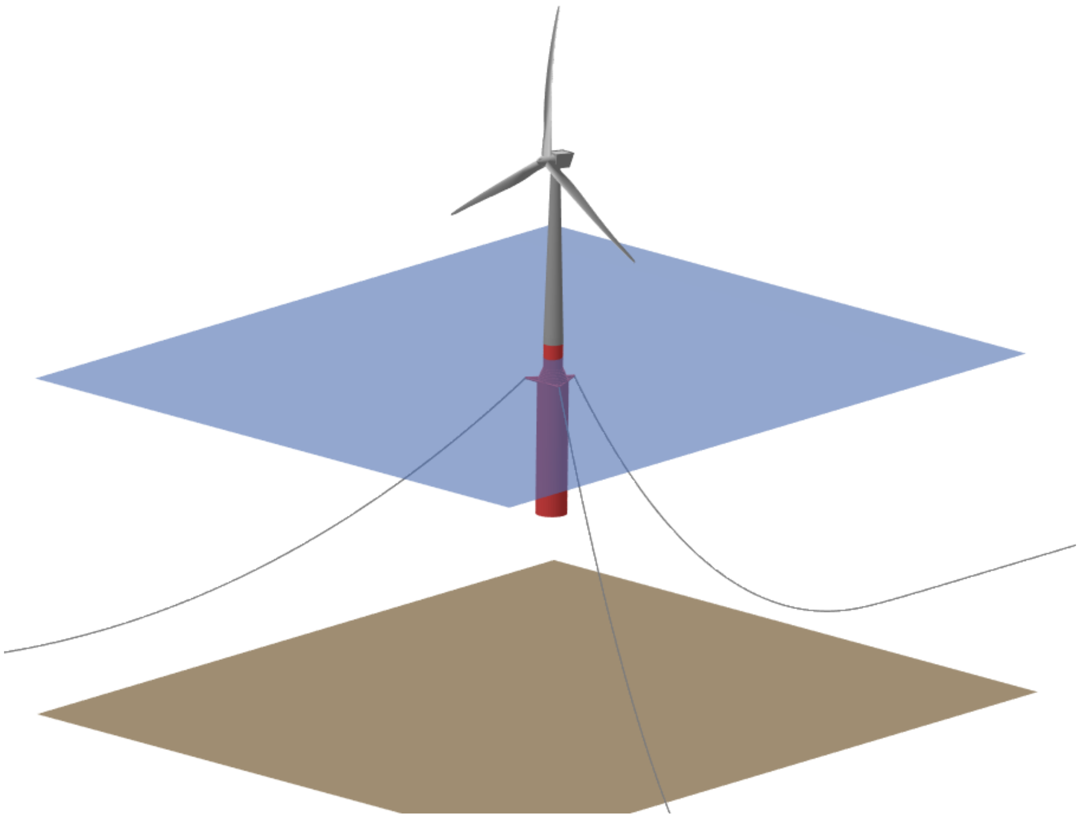

Figure 3. Modified mooring line configuration after optimization aimed at yaw response improvement for AWM control.

Table 1. Mooring configuration for the original Softwind case and for the modified Softwind case optimized for AWM control

	Original configuration	**Modified configuration**
Overall arrangement	Three mooring lines with bridles and delta connection point	Three simple mooring lines
Mooring line length (m)	732 m (*)	683.3 m
Fairlead height	-13.4 m	-12.3 m
Fairlead radial position (*distance from tower axis*)	10.4 m	16.3 m

(*) the total length of a single line here reported is defined summing the length of the mooring line after the delta connection and the length of the two bridles (636 + 48*2= 732 m) between the fairlead and the delta connection point.

It can be noted that the optimization process has affected mainly the position of the fairleads, which has been moved outward from the yaw axis. Such variation has an effect on the sizing of the fairlead support structure, that has been, however, neglected in the present analysis.

5.2.2 Mooring cost estimation

Once the modified mooring configuration has been defined to comply with the control requirements, a further adjustment of the mooring system may be necessary in order to match the load variations determined from the simulations. The required variation of the chain section has been estimated with a size adjustment procedure similar to the general scheme introduced for the other considered components. In particular, the chain nominal diameter d_c (the diameter of the steel bar from which the links of the chain are formed), which is related to the main mechanical properties of the chain line, has been calculated in order to preserve the safety margin of the original configuration. Expressions for the minimum breaking load and fatigue characteristics suggested by widely used marine standards (such as [16]) have been used. Details on the procedure are provided in deliverable D5.1 [5].

5.3 OTHER COST RELATED ASSUMPTIONS

In the approach applied in this study, for the components not involved in the design revision process, the relations between the characteristic system dimensions and the costs have been estimated using typical expressions found in literature. More details on the assumptions on cost modelling can be found in [5] [12] [14] [13].

6 SIMULATION RESULTS

In the proposed methodology for LCOE analysis, a simulation-based approach is used in two different phases of the study:

- DLC1.2 results obtained in Floatech WP2 have been used to estimate a reference power curve for comparison purposes; moreover, some of the results obtained in WP5 for the AWC baseline case (described in deliverable D5.1), where no innovative control is applied, have also been used in this study to define a set of reference data for the above rated conditions; the results from WP2 and WP5 AWC analyses have shown a relatively good agreement, particularly in terms of power output performance;

- for below rated conditions, the results from a Qblade simulation model, implementing the AWM control strategy, have been used to evaluate load and power curve variations with respect to the baseline case.

The need for using data from other phases of the study, for the above rated conditions, is related to the behaviour of the considered control strategy: the AWM control is, in fact, intended to be used only below rated, where the effect of wake interaction is generally larger, due to the generally larger thrust coefficient values, and where less conflicts with the normal pitch control strategy can be expected. Moreover, the implementation of the Helix control strategy is still at a preliminary development stage and does not allow its application to an extended set of DLC simulations, as discussed in the next section.

6.1 AWM SIMULATION CASES AND MODEL SETUP

The behaviour of the Helix control technique, applied to the DTU 10 MW turbine mounted on the Softwind spar buoy platform, has been investigated considering a set of simulations performed using the QBlade code. Due to the early stage of development of the controller, only a relatively reduced set of simulations has been considered. In particular, only the normal power production conditions have been examined, represented by the DLC1.2 as defined by IEC 61400-3 standard [17]. However, the most significant effect of the examined control system is expected during the power production phase of the turbine operation, thus it is expected, also, that the most interesting results for the evaluation of control behaviour can be obtained from the analysed cases.

Moreover, the Helix control technique is applied only in the below rated conditions (in this study around 11 m/s). In fact, at above rated wind speeds, a progressive reduction of the thrust coefficient (related to wake losses) can be generally observed and the wake effects tend to be progressively reduced as well, thus reducing the need for the wake recovery enhancement attainable using the Helix control.

The simulated conditions are, then, restrained to the below rated conditions of the DLC 1.2. For the above rated wind speeds, the results from the same DLC 1.2 with the standard pitch control implementation for maximum power limitation have been used to determine the power curve over the whole operating wind speed range (between cut-in and cut-out wind speeds). The above rated data have been retrieved from the full set of DLC 1.2 simulations used for the AWC control examined in task 5.1 [5].

As already indicated in 5.2.1, the mooring system used in the model has been redesigned, starting from the original model used in WP2, in order to improve the floater response under the action of the Helix control. Such control optimized mooring configuration will be used for the analyses performed in this study.

It has to be noted that, as already remarked, the model used in this analysis to implement the Helix control strategy is essentially oriented to investigate the effect of the blade pitch oscillations on the wake recovery behaviour. Moreover, this model is intended to be used only in the below rated conditions, where the considered control strategy is expected to be applied with higher effectiveness; as such, this preliminary control model does not account for other control issues (such as power limitation) and will probably provide less accurate estimate around the rated wind speed. The preliminary nature of the model is, nonetheless, deemed to be adequate to the overall approach of the present study, which is intended to define an exploratory analysis of the costs and energy production characteristics of the examined designs.

6.2 POWER CURVE FOR THE BASELINE CASE

Using the results of the simulations gathered during Floatech WP2, publicly available on a Zenodo repository [18] [19], a set of reference power production data have been estimated. Results are available for a set of combined environmental conditions (wind and waves, accounting for possible misalignment), representing a possible offshore installation site (West of Barra site) in normal operating conditions (suitable for the estimation of average power production performance). Based on the simulated power output results, an estimate of the power curve of the isolated FOWT (assuming no wake interactions with other turbines) has been obtained using a classic binning approach, complying with typical standard procedures (as described in [17]). This result has been used as a reference also for the analysis of task 5.1 (as reported in deliverable D5.1 [5]).

In the power curve estimation procedure, the simulation results are binned with respect to the wind speed, considering binning intervals of 2 m/s spanning the operating conditions range from 5 m/s (close to the cut-in wind speed) to 25 m/s (close to the cut-off wind speed). In each bin, the wind speed and power output are averaged, yielding the estimated power curve, shown in the following table and figure.

The cut-in and cut-out wind speeds have been assumed equal to 4 m/s and 26 m/s, according to [20].

Table 2. Power curve from simulated normal operating conditions (DLC 1.2). Reference curve from WP2 analyses. "WP2 Reference".

Wind speed WS (m/s)	Mean Power P_{avg} (kW)	Power std dev (kW)
5.1	1003.7	43.8
7.2	2735.2	69.7
9.2	5601.2	131.1
11.2	9437.8	151.8
13.3	10033.0	21.0
15.3	10012.7	6.9
17.3	10002.1	7.4
19.3	9997.4	7.1
21.4	9979.2	5.8
23.4	9973.5	12.9
25.5	9984.6	5.7

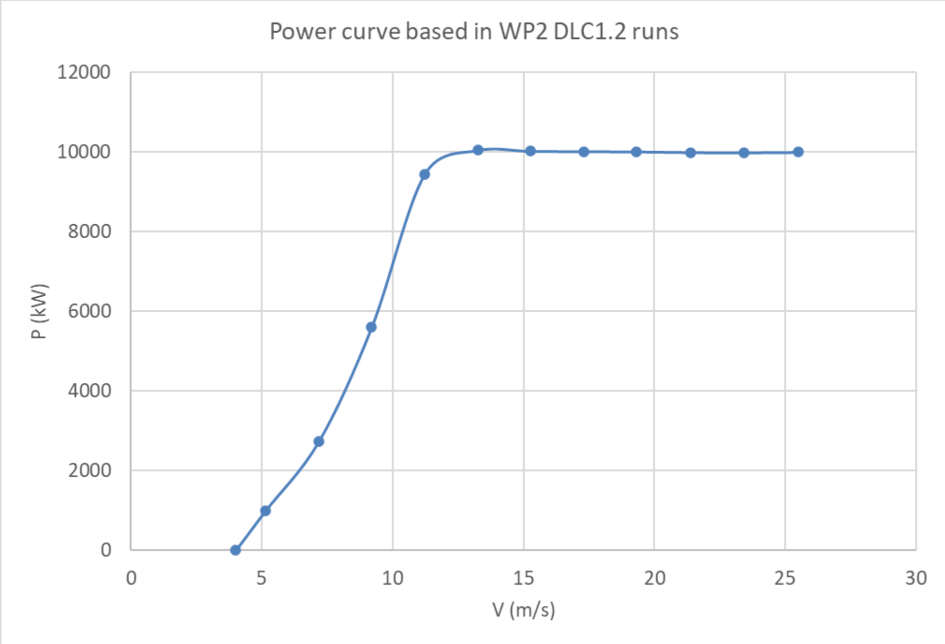

Figure 4. Power curve from simulated normal operating conditions (DLC 1.2).

6.3 SIMULATION RESULTS FOR ACTIVE WAKE MIXING

Using the control developed in WP3, implementing the Helix control strategy for wake recovery enhancement, a set of simulations has been performed and the simulated power output has been used to estimate the related power curve.

6.3.1 Preliminary analyses and results on wake behaviour

A preliminary study has been performed by TU Delft in order to determine the optimal operational parameters for the Helix control. The Helix control introduces a cyclic variation of the blade pitch angle with a given excitation frequency, as shown in [4], which is able to promote an anticipated wake velocity recovery. The choice of the excitation frequency, generally depending on wind speed, is of primary importance for the effectiveness of the control action. The Strouhal number is a parameter generally used in order to express the nondimensional frequency accounting for the variation of wind speed and the geometric size of the rotor. The Strouhal number is defined in this study as follows:

$$St = \frac{f_e D}{U} \tag{3}$$

where f_e is the blade pitch excitation frequency, D is the rotor diameter ($D = 178.3$ m), U is the wind speed. Moreover, the effect of the control on wake recovery is generally variable with the distance behind the turbine.

Accounting for these effects, a set of analyses at a fixed wind speed, equal to 9 m/s, considered as a reference case, has been analysed, changing the excitation frequency and observing the wake recovery at different distance behind the turbine. The following figures, prepared in cooperation with the TU Delft team, show the results for the examined cases, reporting for different values of the Strouhal number the ratio of the speed in the wake at a given distance behind the turbine normalized with respect to the velocity in the wake when the control is inoperative.

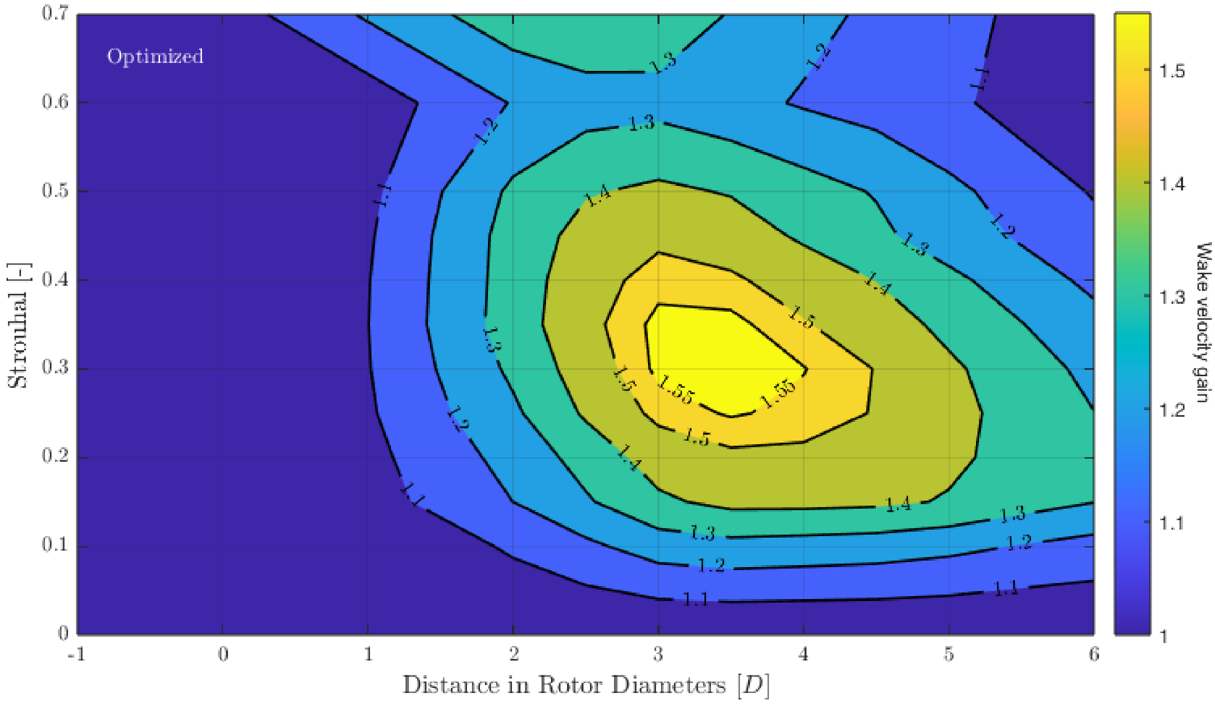

Figure 5. Ratio of the velocity in the wake with Helix control to the velocity in the wake without the control for the optimized configuration, as a function of the distance behind the rotor and of the Strouhal number.

It can be seen that the maximum gain in wake velocity recovery is obtained for an optimal value, St_{opt}, of the Strouhal number equal to about

$$St_{opt} = 0.3$$

It can also be seen that the effectiveness of the control technique in improving wake recovery is variable as a function of the distance behind the rotor, with the maximum improvement being reached in a range of about 3 to 4 rotor diameters of downwind distance.

Based on such results, a variable activation frequency of the blade pitch has been assumed for the simulations, changing as a function of average wind speed and preserving a constant value of the Strouhal number, equal to the estimated optimum value. The assumed blade pitch excitation frequencies are shown in the following table as a function of wind speed.

Table 3. Assumed relationship between blade excitation frequency and wind speed for optimal Helix control operation at constant Strouhal number.

Wind speed (m/s)	Blade pitch excitation frequency (Hz)
3.0	0.005
5.0	0.008
7.0	0.012
9.0	0.015

Moreover, the results of this preliminary investigation on wake effects will also be used to estimate the wake losses due to wake interaction in a farm, that will be later used for energy production and LCOE estimation. Once estimated the optimal value of the Strouhal number, it is assumed that the wake velocity recovery can be considered constant as the Strouhal number is kept constant. The wake velocity deficit, δ, defined as

$$\delta = \frac{U_w - U_\infty}{U_\infty} \tag{4}$$

with U_w velocity in the wake and U_∞ free stream velocity, is shown in Figure 6. The figure shows the trend of wake deficit as a function of the downwind distance for the baseline configuration (with Helix control inactive) compared to the wake deficit with Helix control for both the original mooring configuration and the optimized mooring system. It can be seen that there is an effective improvement of wake recovery, which is amplified by the choice of an optimized mooring line system. It is worth to note, however, that this result is strictly related to the particular choice of the overall floating turbine configuration, namely a spar buoy type platform configuration. Other investigations, applied to different platform types, showed very different results. However, they are not reported here as that is outside the scope of this study.

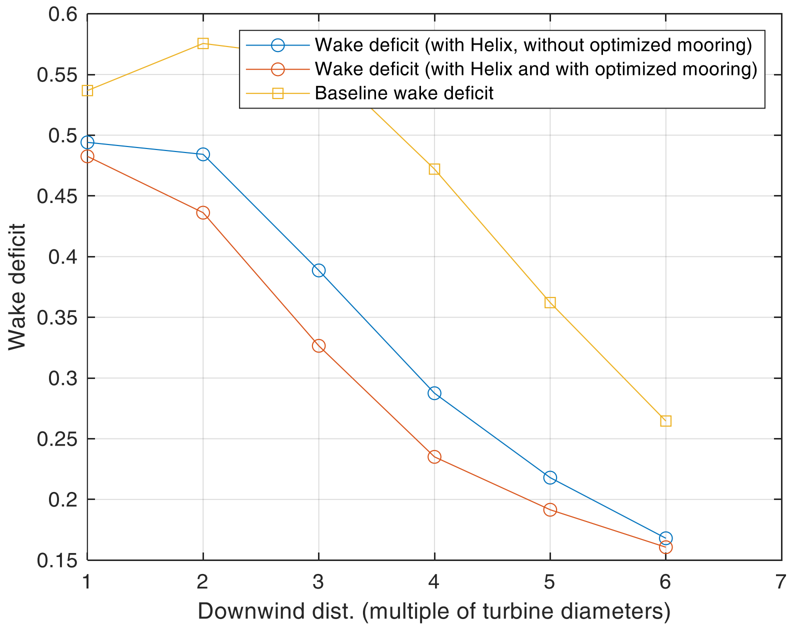

Figure 6. Wake velocity deficit as a function of downwind distance behind the turbine, for St=0.3. The figure shows the baseline wake deficit (without the use of Helix control) compared to the wake deficit with the Helix control with the original mooring configuration and with the optimized mooring system.

6.3.2 Power curve for the optimized configuration with Helix control

The following figures report a set of results derived from the DLC1.2 simulations for the optimized configuration compared to the reference case.

Table 4. Power curve estimated from the simulated normal operating conditions (DLC 1.2) with the Helix control active.

Wind speed WS (m/s)	Mean Power P_{avg} (kW)
4.0	0.0
5.2	1102.0
7.2	2873.6
9.3	5796.2
11.3	10022.7
13.3	9949.6
15.3	9996.4
17.4	9999.2
19.4	10004.1
21.4	9998.3
23.6	9994.3
26.0	9994.3

It can be seen that the output power slightly overcome the power output estimated for the original control solution close to the rated wind speed; the output power level has been set equal to the rated power level (10 MW) in the power curve used to estimate energy production, as shown in the figure. A further tuning of the control is needed to avoid exceeding the generator power limit.

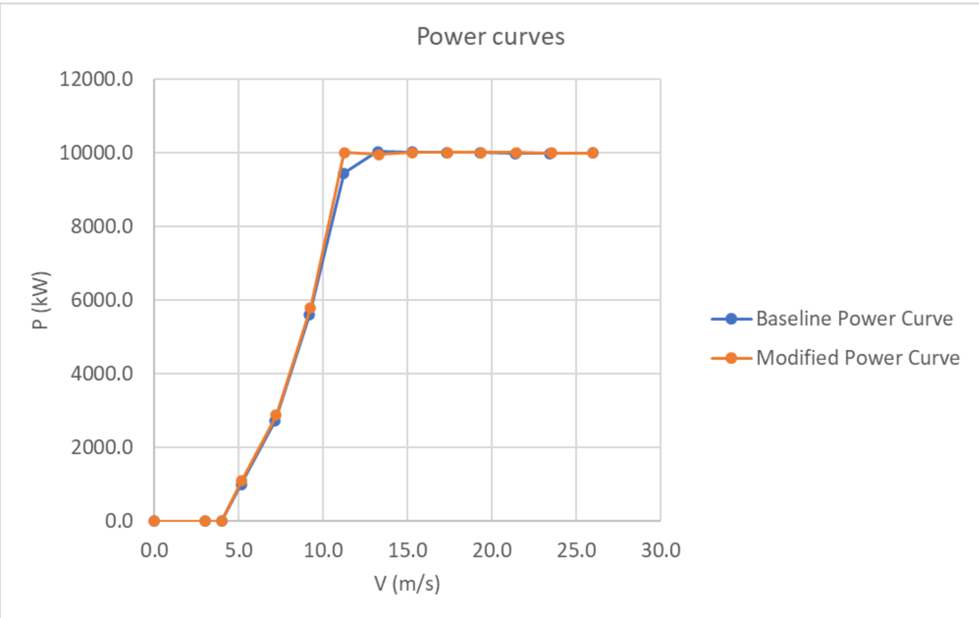

Figure 7. Power curve for Helix control from DLC1.2 simulations (compared to the reference case without Helix control).

6.3.3 Thrust coefficient

The analysis of the simulation data also allows to determine the variation of the thrust coefficient with wind speed. The following figure shows a comparison between the thrust coefficient with and without the Helix control.

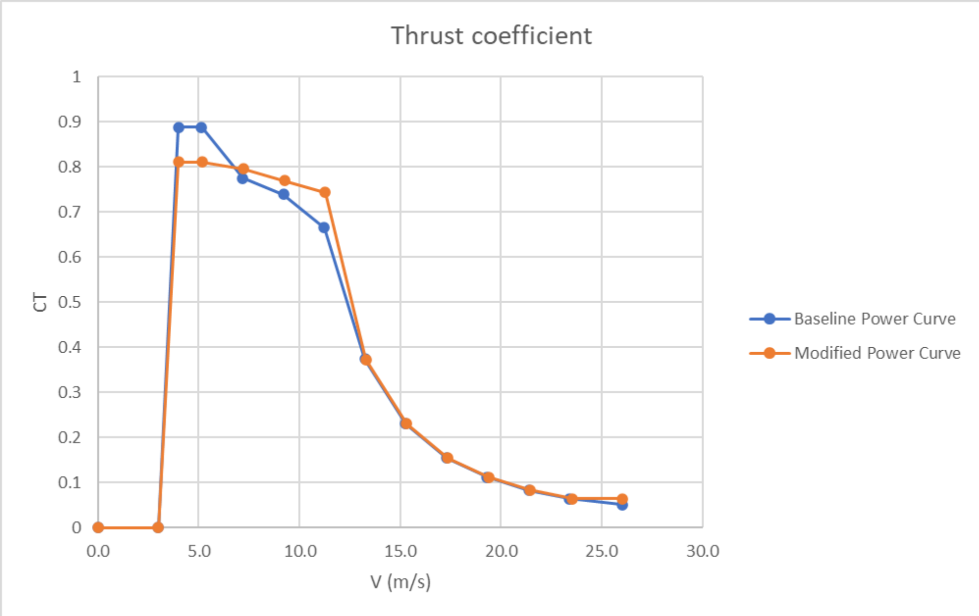

Figure 8. Thrust coefficient as a function of wind speed for the AWM Helix control technique, compared to the Baseline case, from WP2 simulations.

6.3.4 DEL variation

Using simulation results it has been possible to determine the Damage Equivalent Loads (DELs) for both the configurations tested. The comparison between the cases with and without Helix control is summarized in the following table.

Table 5. DEL loads variations for the Softwind case, with/without Helix control strategy.

idx	Label	Units	Softwind Baseline	Softwind AWMHelix	AWMHelix - Baseline diff. (%)
RootMxb1	B1 Root Mx	[Nm]	44281.0	41925.0	-5.321%
RootMyb1	B1 Root My	[Nm]	18229.0	18229.0	0.000%
RootMzb1	B1 Root Mz	[Nm]	37370.0	36964.0	-1.086%
RootMxb2	B2 Root Mx	[Nm]	44274.0	41909.0	-5.342%
RootMyb2	B2 Root My	[Nm]	18211.0	18211.0	0.000%
RootMzb2	B2 Root Mz	[Nm]	37313.0	36880.0	-1.160%
RootMxb3	B3 Root Mx	[Nm]	44332.0	41979.0	-5.308%
RootMyb3	B3 Root My	[Nm]	18219.0	18219.0	0.000%
RootMzb3	B3 Root Mz	[Nm]	37312.0	36825.0	-1.305%
YawBrFxp	TT Fx	[N]	267120.0	277500.0	3.886%
YawBrFyp	TT Fy	[N]	109330.0	182920.0	67.310%
YawBrFzp	TT Fz	[N]	50253.0	71154.0	41.592%
YawBrMxp	TT Mx	[Nm]	1236200.0	1314100.0	6.302%
YawBrMyp	TT My	[Nm]	3824700.0	9426800.0	146.472%
YawBrMzp	TT Mz	[Nm]	3754800.0	8131800.0	116.571%
TwrBsFxt	TB Fx	[N]	398830.0	442680.0	10.995%
TwrBsFyt	TB Fy	[N]	211450.0	397090.0	87.794%
TwrBsFzt	TB Fz	[N]	52552.0	72820.0	38.568%
TwrBsMxt	TB Mx	[Nm]	16398000.0	28502000.0	73.814%
TwrBsMyt	TB My	[Nm]	34347000.0	38350000.0	11.655%
TwrBsMzt	TB Mz	[Nm]	3729800.0	8147900.0	118.454%
FAIRTEN1	FAIRTEN1	[N]	154280.0	140200.0	-9.126%
FAIRTEN2	FAIRTEN2	[N]	186580.0	189650.0	1.645%
FAIRTEN3	FAIRTEN3	[N]	195390.0	196920.0	0.783%

It is possible to note a large variation for some of the considered load components. In particular, regarding blade loads, it can be seen a noticeable decrease in the edgewise blade root bending moment. The largest percentage variation, however, can be seen for the tower loads, as expected due to the additional periodic moments generated by the cyclic variation of blade pitch. Due to the yawing action generated by the Helix control, a large increase can be seen for the torsional action on the tower; nonetheless, according to the preliminary nature of this analysis, the design of the tower has been considered mainly influenced by the bending moments and the torsional actions have been neglected, being in general less demanding for the section design. Substantial variations, however, have also been observed with respect to the tower bending moments, which can affect tower sizing and the related costs. The tower base loadings can also affect the sizing of the floater structure and the related costs. Smaller variations can be observed for the mooring line tensions; in this case, a slight reduction in tension can be seen for the downwind line, while even slighter increase can be seen on the other two upwind lines.

In this study only a small set of normal production simulations has been carried out, due to the control implementation, which allowed its application only to the below rated conditions. The Helix control strategy has been, in fact, conceived to be used only below rated, where larger thrust coefficients can, in general, be seen and the wake deficit effects can be more significant. For above rated wind speeds results for the baseline simulations have been used. Maximum loads, moreover, have been considered unchanged by the presence of the control; this assumption is motivated based on the fact that the control is activated in normal operating conditions, while, generally, peak loads are associated to extreme conditions. Max loads have been retrieved from the baseline simulation results. Of course, this assumption implies a strong simplification, approximately acceptable at a preliminary stage, but requiring further verifications for the definition of the final design.

These results have been used in the cost estimation model to evaluate the component cost variation associated to the change in control strategy. The following table shows a summary of the load variations considered for the analyses. The combined M_{xy} blade root moment DEL has been estimated as an average of the DELs for each blade. For the mooring lines, the maximum DEL variation has been considered.

Table 6. Load variations considered in the analysis.

Moorings	**Baseline**	**Modified**	**Variation**
Tension DEL (kN)	195.4	196.9	0.8%
Tension MAX (kN)	4296.8	4296.8	0.0%
Platform	**Baseline**	**Modified**	**Variation**
Tower base moment DEL (kNm)	38060.6	47781.7	25.5%
Tower base moment MAX (kNm)	1058338.7	1058338.7	0.0%
Blade	**Baseline**	**Modified**	**Variation**
Blade root moment (kNm) DEL	47933.5	45766.1	-4.5%
Blade root moment (kNm) MAX	74891.2	74891.2	0.0%
Tower	**Baseline**	**Modified**	**Variation**
Tower top force DEL (kN)	288.6	332.4	15.15%
Tower top force MAX (kN)	6524.8	6524.8	0.00%

7 ANNUAL ENERGY PRODUCTION

7.1 SITE CHARACTERISTS

In order to estimate the Annual Energy Production, some assumptions on the wind speed distribution have been made. The wind climate at the West of Barra site has been considered. This site has already been used in the Work Package 2 of the Floatech project. Data related to the climate of this site can be found in [21] [22]. For the purpose of this study, a joint distribution of wind speed magnitude and direction will be considered in order to take into account the combined variability of wind speed and direction. The data used for the analyses here reported are shared with the deliverable D5.1 [5].

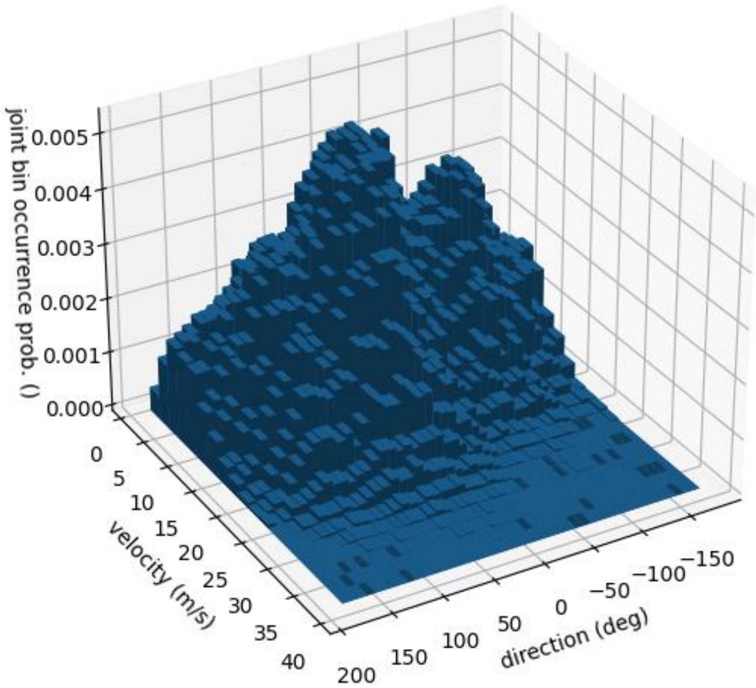

Figure 9. Joint distribution of wind speed and direction (West of Barra site). (The reported directions represent the directions towards which the wind is oriented).

7.2 FARM LAYOUT AND WAKE MODELLING ASSUMPTIONS

Once the wind climate has been described through an occurrence probability matrix for the combination of wind speed magnitude and direction, a farm layout has to be specified so that the effect of wake interaction between each pair of turbines in the plant can be estimated for each incoming wind direction. To evaluate the wake interaction between turbines, the wake velocity deficit has to be described as a function of wind speed and of the relative distance of the FOWTs. The wake velocity deficit can be estimated using engineering models. In this study, moreover, the results obtained from the QBlade simulations will be used to determine the flow characteristics in the wake behind a turbine, accounting for the possible effect of AWM control strategy.

The overall energy production for the assumed layout can then be estimated, allowing the evaluation of the LCOE in the two compared scenarios (with/without AWM).

The effect of the AWM control (in the form of the Helix control strategy) is dependent on the wind farm layout and on the number of installed FOWTs, which affect the overall wake interaction losses. Thus, in order to study the impact of the control strategy on the farm LCOE, some assumptions on the farm geometrical features have to be accepted: in this study a square distribution of the turbines is considered, as illustrated in Figure 10.

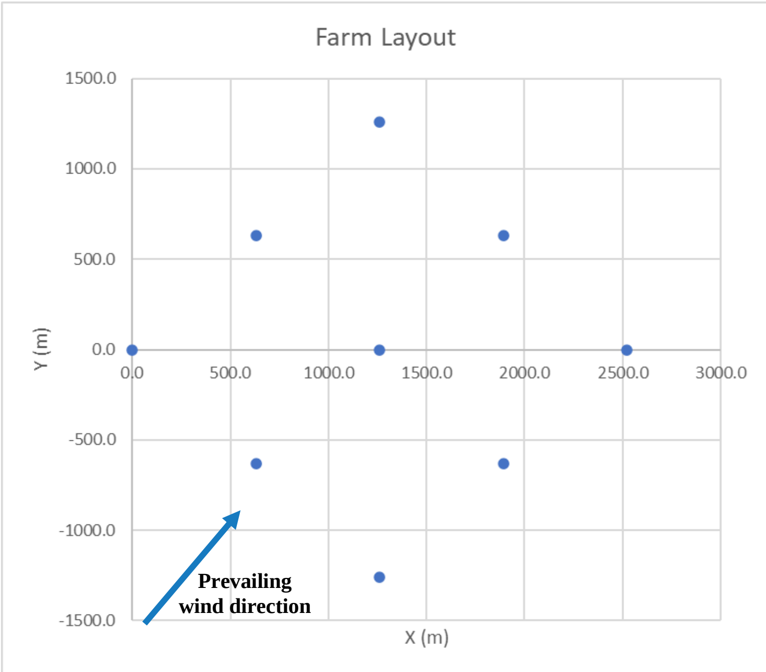

Figure 10. Assumed farm layout (the number of turbines is varied in a parametric study).

The distance between the turbines is also assumed constant, in both the directions (lines and rows), and equal to a given multiple of the rotor diameter, D. Throughout the study, the nondimensional turbine distance, Λ, has been assumed equal to

$$\Lambda = 5D$$

In the case of multiple turbines, wake effects from different turbines may superimpose on the trailing units for a given wind direction. In such cases, a superposition formulation has to be assumed in order to estimate the combined effect: in this study, an approach based on the squared sum combination method, widely used in classical engineering models for wake interaction, has been applied. It is assumed that, when more than one upwind turbine wakes affect a trailing turbine, the overall wake velocity reduction can be expressed as follows

$$\delta_i^2 = \sum_{j=1}^{n} \delta_{ij}^2 \tag{5}$$

where δ_i represents the overall wake velocity deficit (defined in 6.3.1) on the i-th turbine in the farm, determined by the superposition of each of the wake effects, δ_{ij}, from the generic j-th interacting turbine on the i-th downwind unit. The wake deficit δ_{ij} can expressed as a function of the wind speed and of the distance behind the upwind turbine; in this study, we assume that the wake deficit can be represented in a matrix form, as indicated in the following tables for the two cases with and without control.

Table 7. Assumed wake deficit as a function of wind speed and distance for the Baseline case (without Helix control strategy).

Baseline wake deficit								
Wake deficit	**Distance behind the turbine (multiple of rotor diameter)**							
Wind speed Vm (m/s)	**2**	**3**	**4**	**5**	**6**	**15**	**25**	**50**
1.0	0.00	0.00	0.00	0.00	0.00	0.00	0.00	0.00
3.0	0.00	0.00	0.00	0.00	0.00	0.00	0.00	0.00
5.0	0.51	0.36	0.28	0.22	0.18	0.05	0.02	0.01
7.0	0.55	0.38	0.28	0.22	0.18	0.05	0.02	0.01
9.0	0.54	0.37	0.27	0.21	0.17	0.05	0.02	0.01
11.0	0.50	0.35	0.26	0.20	0.16	0.04	0.02	0.01
13.0	0.31	0.22	0.16	0.13	0.10	0.03	0.01	0.00
15.0	0.18	0.13	0.10	0.08	0.06	0.02	0.01	0.00
17.0	0.12	0.09	0.07	0.05	0.04	0.01	0.00	0.00
19.0	0.00	0.00	0.00	0.00	0.00	0.00	0.00	0.00
21.0	0.00	0.00	0.00	0.00	0.00	0.00	0.00	0.00
23.0	0.00	0.00	0.00	0.00	0.00	0.00	0.00	0.00
25.0	0.00	0.00	0.00	0.00	0.00	0.00	0.00	0.00
28.0	0.00	0.00	0.00	0.00	0.00	0.00	0.00	0.00
32.5	0.00	0.00	0.00	0.00	0.00	0.00	0.00	0.00
37.5	0.00	0.00	0.00	0.00	0.00	0.00	0.00	0.00

Table 8. Assumed wake deficit as a function of wind speed and distance for the Modified case (with Helix control strategy).

Baseline wake deficit								
Wake deficit	**Distance behind the turbine (multiple of rotor diameter)**							
Wind speed Vm (m/s)	**2**	**3**	**4**	**5**	**6**	**15**	**25**	**50**
1.0	0.00	0.00	0.00	0.00	0.00	0.00	0.00	0.00
3.0	0.00	0.00	0.00	0.00	0.00	0.00	0.00	0.00
5.0	0.39	0.21	0.14	0.12	0.11	0.03	0.01	0.00
7.0	0.42	0.22	0.14	0.12	0.11	0.03	0.01	0.00
9.0	0.41	0.21	0.14	0.11	0.10	0.03	0.01	0.00
11.0	0.38	0.20	0.13	0.11	0.10	0.03	0.01	0.00
13.0	0.31	0.13	0.08	0.07	0.06	0.02	0.01	0.00
15.0	0.18	0.08	0.05	0.04	0.04	0.01	0.00	0.00
17.0	0.12	0.05	0.03	0.03	0.03	0.01	0.00	0.00
19.0	0.00	0.00	0.00	0.00	0.00	0.00	0.00	0.00
21.0	0.00	0.00	0.00	0.00	0.00	0.00	0.00	0.00
23.0	0.00	0.00	0.00	0.00	0.00	0.00	0.00	0.00
25.0	0.00	0.00	0.00	0.00	0.00	0.00	0.00	0.00
28.0	0.00	0.00	0.00	0.00	0.00	0.00	0.00	0.00
32.5	0.00	0.00	0.00	0.00	0.00	0.00	0.00	0.00
37.5	0.00	0.00	0.00	0.00	0.00	0.00	0.00	0.00

The values indicated above for the wake losses have been determined using the following procedure: the assumed wake deficit values for the baseline case (reported in Table 7) are based on the max wake deficit for a gaussian wake model [23] [24], already described in D5.1, while the wake deficit values for the modified case, reported in Table 8, are obtained by reducing the gaussian wake deficit according to the results of the simulations. In particular, the values of the modified wake deficit (Table 8) have been derived from the baseline values (Table 7) using a scaling ratio equal to the ratio between the Helix wake deficit and the baseline wake deficit obtained from the preliminary simulation and shown in Figure 6. The values assumed to define the ratio between the wake deficit with and without Helix are reported in the following table (and also shown in Figure 11). The ratio has been conservatively considered constant after 6 diameters in lack of data for larger distance; however, it is assumed that for very large distance the wake interaction effects tend to be progressively smaller, reducing the consequences of such simplified assumption.

Table 9. Wake deficit ratio with/without Helix at 9 m/s as a function of the distance behind the rotor.

Downwind distance (multiple of rotor diam.)	***Wake deficit ratio***
2	0.7579
3	0.5794
4	0.4979
5	0.5288
6	0.6072
15	0.6072
25	0.6072
50	0.6072

The use of such approximate scaling approach for the estimation of the wake deficit is aimed to extended the availability of wake deficit data, originally available only for a single wind speed, to the full range of wind speed observed in the considered site.

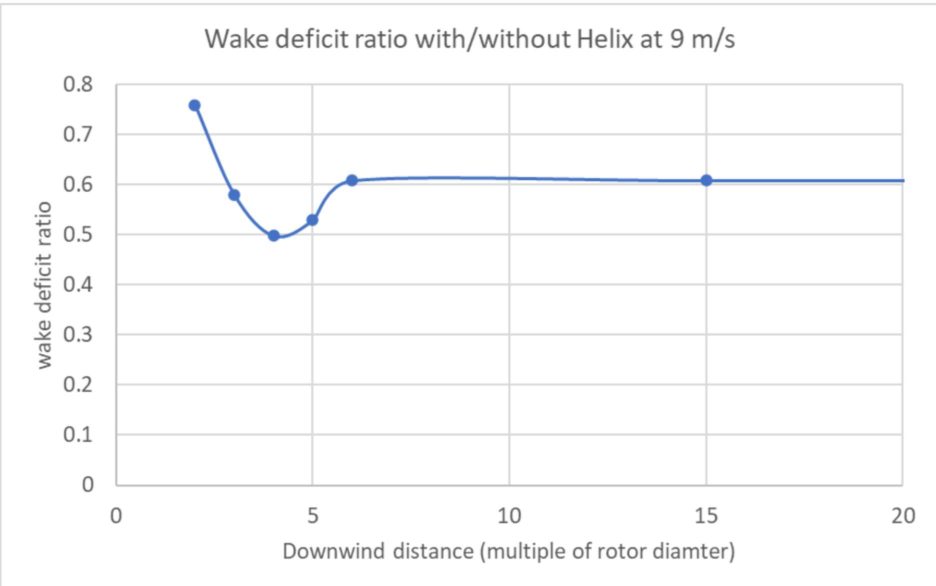

Figure 11. Wake deficit ratio with/without Helix at 9 m/s as a function of the distance behind the rotor.

8 ESTIMATION OF LCOE VARIATION

8.1 LCOE VARIATION WITH HELIX CONTROL STRATEGY. EFFECT OF FARM SIZE

Based on the results of the simulations, the variation of the LCOE value can be estimated, accounting for both the variation of the component costs, related to the structural mass variation, and the variation of the annual energy production, between the baseline configuration (without AWM control) and the modified configuration (with AWM control).
Assuming the layout described in 7.2, a set of LCOE values can be estimated for different numbers of wind turbines with the same spatial distributions. The following table and figure gather the data estimated for the assumed layout.

Table 10. Effect on LCOE of the farm size. Percent reduction of LCOE with/without control.

n. rows	n. lines	n. turbines	AEP w/o Helix (MWh/year)	AEP w Helix (MWh/year)	LCOE w/o Helix (€/MWh)	LCOE w Helix (€/MWh)	LCOE reduction
1	1	1	54763	55572	175.42 €	174.11 €	-0.75%
2	2	4	209902	217108	169.60 €	165.15 €	-2.62%
3	3	9	458775	480340	172.02 €	165.49 €	-3.80%
4	4	16	800149	844540	174.43 €	166.46 €	-4.57%
5	5	25	1233886	1309615	176.31 €	167.32 €	-5.10%
6	6	36	1759915	1875521	177.76 €	168.02 €	-5.48%
7	7	49	2378119	2542181	178.91 €	168.58 €	-5.77%

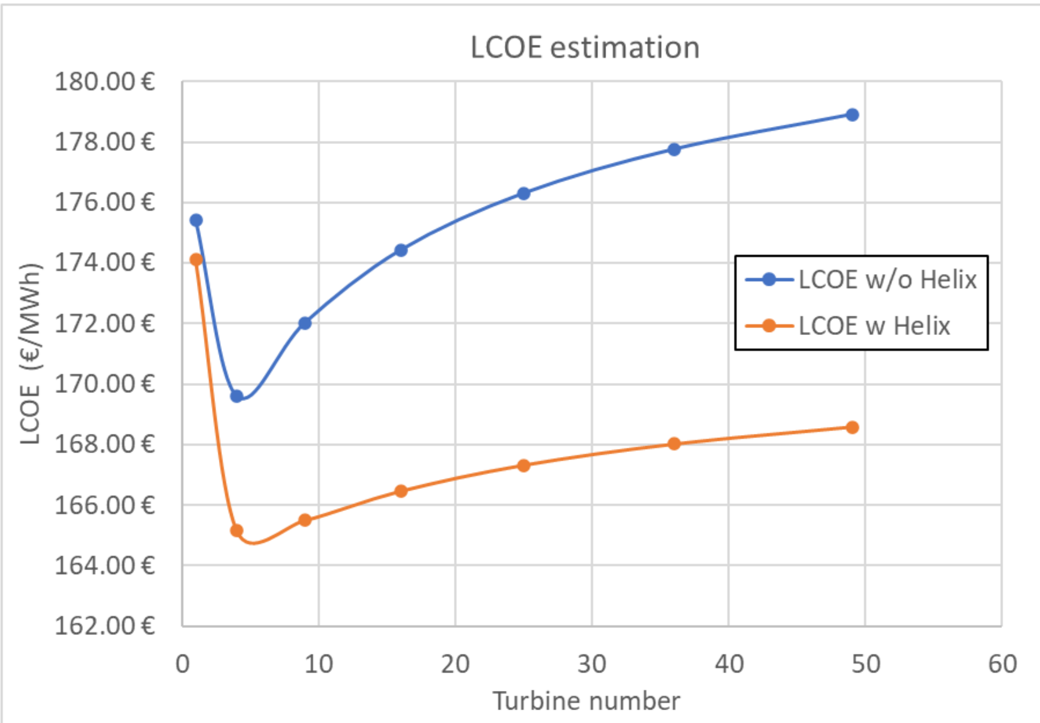

Figure 12. Variation of LCOE estimation as a function of the number of FOWT units in the farm, with and without the AWM control strategy.

It can be seen from Figure 12 that the estimated value of LCOE without the AWM control strategy, shows a range of variation between about 170 €/MWh and 179 €/MWh in the baseline case. On the other hand, in the case with the AWM control, lower LCOE values can be observed over the whole explored range of farm size, varying between about 165 €/MWh and 174 €/MWh. It can also be noted a similar behaviour in the overall trends: the LCOE shows a decrease trend initially, for small farm sizes, until a minimum value is reached. Based on the previous figure, with the AWM control, the LCOE values show a reduction compared to the baseline over the whole considered range of farm sizes, and the increase in LCOE after the minimum is less pronounced. This increasing trend for large farm size may be related to the suboptimal simplified layout assumed for this analysis (whose purpose is to provide a preliminary estimation), with a relatively small distance between the installed turbines. These conditions can lead to a nonnegligible worsening of the wake interaction effects for an increasing number of installed units, non-optimally distributed in the farm area.

It can, also, be noted (Figure 13) that there is a nonnegligible improvement in LCOE with the AWM control. The figure shows the percent variation of the LCOE between the configurations with and without the control: progressively larger reduction of the LCOE can be observed for increasing number of turbines, at least in the explored range of farm sizes. The maximum LCOE reduction among the considered cases, equal to slightly less than -6%, is reached for the 7x7 farm size, for the assumed layout. The trend of the LCOE reduction rate for increasing farm sizes seems to be progressively smaller. This trend seems to suggest a tendency towards an asymptotic value. However, the accuracy of the simple wake interaction model assumed in the analysis, which affects LCOE estimation particularly for this type of control strategy, is questionable for very large farm sizes. A small reduction in LCOE can be seen also for the single turbine case, mainly due to a slight increase in energy production obtained due to a slight increase in the power curve derived from the analysis of the DLC1.2 simulations (Figure 7), at least for the assumed simplified control implementation used in the analysis.

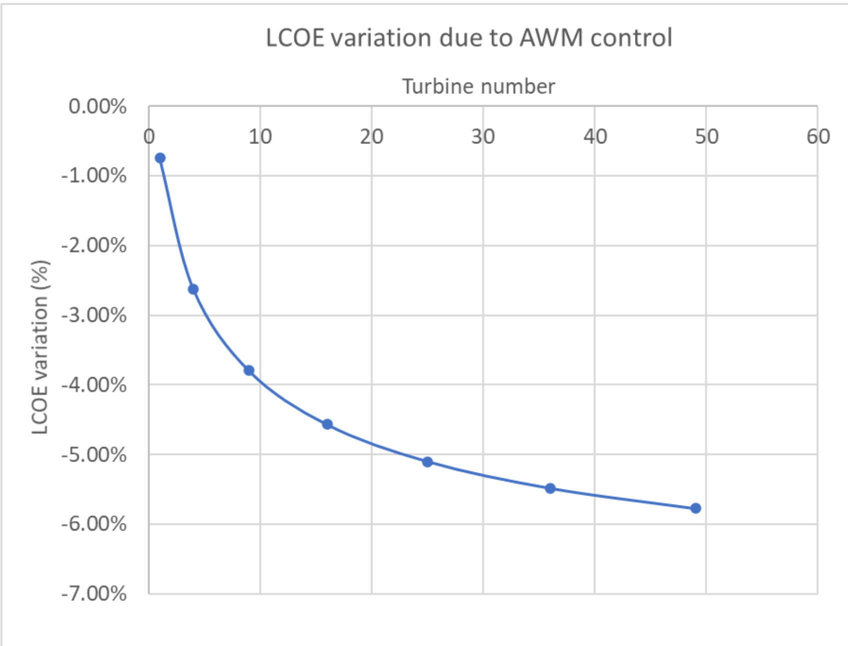

Figure 13. Effect on LCOE reduction of the farm size.
Percent reduction of LCOE between the two configurations with and without the AWM control.

8.2 EFFECT OF THE WIND CLIMATE VARIATION

The particular wind climate may also have an impact on the effectiveness of the considered control strategy. As an example, in order to consider an extreme case, in this study we can consider a fictitious case, based on the West of Barra case, with the same wind speed distributions but with a constant directional distribution, with the wind always oriented as the prevailing wind direction shown in Figure 10. In this theoretical limit case, the effect of the wake interaction is amplified and thus the LCOE reduction predicted by the model is slightly larger than in the case of the direction distribution for the real wind climate. This value is purely theoretical, but it is reported here for comparison purposes, in the example case of a 3x3 farm layout, as a limiting case for estimating the theoretical capability of the control technology in different local weather conditions. The following table shows the expected LCOE values with and without the AWM control.

Table 11. LCOE variation for 3x3 farm layout. Fictitious extreme case with constant wind direction.

	Baseline	**Modified**	
LCOE	187.11 €	172.95 €	€/MWh
LCOE variation		-7.57%	

It can be seen, that in this limiting case, the LCOE reduction reaches, as expected, a larger value compared to the case with a more realistic wind direction distribution, passing from a value of about -4 % to a value of about -8% for the 3x3 farm size.

9 CONCLUSION AND OBSERVSATIONS

The application of the developed simplified cost and energy production model shows some encouraging results for the Helix control strategy. The methodology has some limitations, mainly related to the limited number of considered components and to the reduced set of simulations taken into account in the study (essentially limited to the normal production conditions), even if it should be considered that these are the most frequent working condition of the turbines. Nonetheless, at least in the preliminary perspective of this study, a significant improvement may be observed, mainly related to the reduction in wake losses generated by the proposed innovative Helix control strategy. A reduction of the LCOE in the approximate range between -3% and -6% has been observed considering a simplified square farm layout with a variable number of installed units (over a farm size range between 4 and 49). The larger LCOE reductions are observed for the larger farm sizes, probably due to a more significant effect of the wake losses which allows for a more effective exploitation of the wake recovery improvement due to the wake mixing technique.

The results obtained in the present analysis are related to the specific choice of the considered environmental conditions and to the assumed layout. In particular, the distance between the turbines has been set equal to 5 rotor diameters, which is rather smaller than the typical farm spacing according to part of the literature (between 8 and 12 diameters [25]). The reason behind this choice of the spacing was the aim to investigate the effectiveness of the wake recovery improvement for a layout where larger wake effects are expected and thus larger benefits may be earned using the considered innovative control strategy.

Another limitation of the approach used in this study is related to the limited number of simulations used in the analysis, which may affect the accuracy of load estimation and of the related cost evaluation. Nonetheless, the limited amount of simulated data is consistent with the preliminary character of the present comparative study.

The main source of LCOE reduction can be found in the effect of the new control technique on the wake interactions. However, a slight improvement can also be indirectly related to the modification of the mooring line system. In fact, the mooring system has been optimized to operate in combination with the Helix control, maximizing the response of the platform yaw motion under the action of the Helix generated yawing moment. The purpose of the optimization was to increase the yaw response to enhance the induced wake oscillations which are responsible for the expected faster wake speed recovery in the Helix strategy. The optimized mooring configuration obtained in this study has a simple 3-lines arrangement (with no bridles and delta connection) and is characterized by a lower line length, which in turn yields also a slight reduction in the mooring cost. Of course, this effect has to be considered in the limits of the preliminary character of the current analysis. A more detailed study should take into account the effect of such configuration change in an iterative way by considering the effect of all the combined design variations on the loads and on the sizing of the components. Moreover, an iterative design approach should consider the variation of the FOWT response and loadings, possibly induced by the modification of the design parameters, until a convergence criterion is met. However, such iterative study is outside the scope of this work and maybe the subject of further developments in dedicated future research projects.

REFERENCES

[1] Wind-Europe, “Wind energy in Europe,” 2023.

[2] K. Yilmazlar, S. Cacciola, M. Xiolesmy, A. Rodriguez and A. Croce, “Development of engineering cost models for integrated design optimization of onshore and offshore wind farms,” in *The Science of Making Torque from Wind (TORQUE 2022)*, Delft, Netherlands, 2022.

[3] Delft University of Technology, Technical university of Berlin, “An advanced open source wind turbine controller for power generation and load mitigation using real-time feedforward wave information,” Floatech research project, 2022.

[4] J. A. Frederik, B. M. Doekemeijer, S. P. Mulders and J.-W. v. Wingerden, “The helix approach: Using dynamic individual pitch control to enhance wake mixing in wind farms,” *Wind Energy,* no. 23, p. 1739–1751, 2020.

[5] D. Coiro, G. Troise and A. Grieco, “Floatech D5.1 Report on the LCOE improvement of AWC controlled floating wind farms,” Floatech, 2023.

[6] C. Kost, S. Shammugam, V. Fluri, D. Peper, A. D. Memar and T. Schlegl, “LEVELIZED COST OF ELECTRICITY RENEWABLE ENERGY TECHNOLOGIES,” Fraunhofer ISE, Freiburg, 2021.

[7] V. Arnal, «Experimental Modelling of a floating wind turbine using a "software-in-the-loop" approach.,» ECN, Nantes, 2020.

[8] C. Bak, F. Zahle, R. Bitsche, T. Kim, A. Yde, L. C. Henriksen, M. H. Hansen, J. P. A. A. Blasques, M. Gaunaa and A. Natarajan, “The DTU 10-MW Reference Wind Turbine,” DTU Library, 2013.

[9] K. Müller, F. Lemmer and W. Yu, “Deliverable D4.2 Public Definition of the Two LIFES50+ 10MW Floater Concepts - Qualification of innovative floating substructures for 10MW wind turbines and water depths greater than 50m,” Lifes50+ Project, 2018.

[10] H. Ege, “Investigation of the Tower Design for the Offshore Wind Turbine Concept OO-Star Wind Floater,” NTNU Master Thesis, 2019.

[11] S. Perez-Becker and R. B. D. Luna, “D2.1. Aero-Hydro-Elastic Model Definition in QBlade Ocean,” Floatech Project, 2022.

[12] P. Beiter, W. Musial, A. Smith, L. Kilcher, R. Damiani, M. Maness, S. Sirnivas, T. Stehly, V. Gevorgian, M. Mooney and G. Scott, “A Spatial-Economic CostReduction Pathway Analysis Reduction Pathway Analysis for U.S. Offshore Wind Energy Development from 2015–2030,” NREL, 2016.

[13] A. Martinez and G. Iglesias, “Mapping of the levelised cost of energy for floating offshore wind in the European Atlantic,” *Renewable and Sustainable Energy Reviews,* vol. 154, 2022.

[14] S. HEIDARI, Economic modelling of floating offshore wind power. Calculation of levelized cost of energy, Sweden: School of business, society and engineering: Master thesis., 2017.

[15] D. van den Berg, D. de Tavernier and J.-W. van Wingerden, "Using The Helix Mixing Approach On Floating Offshore Wind Turbines," *Journal of Physics: Conference Series,* vol. 2265, 2022.

[16] DNV, "Offshore Mooring Chain DNV-OS-E302," DNV, 2013.

[17] IEC, «IEC 61400-12-1 Wind energy generation systems - Part 12-1: Power performance measurements of electricity producing wind turbines,» IEC, 2022.

[18] F. Papi, R. Behrens de Luna, J. Saverin, D. Marten, C. Combreau, G. Troise, G. Mirra and A. Bianchini, "Deliverable 2.3 Design Load Case Database for Code to Code Comparison," Floatech, 31 10 2022. [Online]. Available: https://zenodo.org/record/7817708.

[19] F. Papi, A. Bianchini, G. Troise, G. Mirra, D. Marten, J. Saverin, R. Behrens de Luna, M.-L. Ducasse and J. Honnet, "Deliverable 2.4 Full report on the estimated reduction of uncertainty in comparison to the state-of-the-art codes OpenFAST and DeepLines Wind," Floatech, 2022.

[20] S. Wang, T. J. Larsen and H. Bredmose, "Ultimate load analysis of a 10 MW offshore monopile wind turbine," DTU Library, 2021.

[21] P. Gómez, G. Sánchez, A. Llana and G. Gonzalez, "Lifes50+ Deliverable D1.1 Oceanographic and meteorological conditions for the design," Lifes50+, 2015.

[22] F. Vigara, L. Cerdán, R. Durán, S. Muñoz, M. Lynch, S. Doole, C. Molins, P. Trubat and R. Guanche, "Corewind project deliverable D1.2 Design Basis," 2020.

[23] M. Bastankhah and F. Porté-Agel, "A new analytical model for wind-turbine wakes," *Renewable Energy,* no. 70, pp. 116-123, 2014.

[24] M. Krutova, M. B. Paskyabi, F. G. Nielsen and J. Reuder, "Evaluation of Gaussian wake models under different atmospheric stability conditions: Comparison with large eddy simulation results," *Journal of Physics: Conference Series,* vol. 1669, p. 012016, 2020.

[25] P. Hou, J. Zhu, K. Ma, G. YANG, W. Hu e Z. CHEN, «A review of offshore wind farm layout optimization and electrical system design methods,» *Journal of Modern Power Systems and Clean Energy,* vol. 7, n. 5, p. 975–986 , 2019.

[26] P. Bortolotti, D. Berry, R. Murray, E. Gaertner, D. Jenne, R. Damian, G. B. and K. Dykes, "A Detailed Wind Turbine Blade Cost Model," NREL, 2019.

[27] A. d. Carvalho, "STEEL MARKET DEVELOPMENTS Q4 2015," OECD, Paris, Fr, 2016.

[28] L. Fingersh, M. Hand and A. Laxson, "Wind Turbine Design Cost and Scaling Model," NREL, 2006.

[29] A. Ghigo, L. Cottura, R. Caradonna, G. Bracco and G. Mattiazzo, "Platform Optimization and Cost Analysis in a Floating Offshore Wind Farm," *Journal of Marine Science and Engineering,* vol. 8, no. 835, 2020.

[30] M. Maness, B. Maples and A. Smith, "NREL Offshore Balance-ofSystem Model," NREL, DENVER (CO), USA, 2017.

[31] A. Myhr, C. Bjerkseter, A. Ågotnes and T. A. Nygaard, “Levelised cost of energy for offshore floating wind turbines in a life cycle perspective,” *Renewable Energy,* vol. 66, pp. 714-728, 2014.

[32] S. Santhakumar, G. Smart, M. Noonan, H. Meerman and A. Faaij, “Technological progress observed for fixed-bottom offshore wind in the EU and UK,” *Technological Forecasting & Social Change,* vol. 182, no. 121856, 2022.

[33] J. N. Sørensen and G. C. Larsen, “A Minimalistic Prediction Model to Determine Energy Production and Costs of Offshore Wind Farms,” *Energies, MDPI,* vol. 14, no. 448, 2012.

[34] H. Ahn, Y.-J. Ha and K.-H. Kim, “Load Evaluation for Tower Design of Large Floating Offshore Load Evaluation for Tower Design of Large Floating Offshore,” *Energies,* vol. 16, no. 1862, 2023.

[35] S. Allegretto, Performance analysis and cost modelling for offshore floating wind turbines, Master thesis, 2021.

[36] OECD, “"Prices: Producer prices"Main Economic Indicators (database),,” 2023. [Online]. Available: https://doi.org/10.1787/data-00535-en. [Accessed 2023 March 30].

[37] W. Kuckshinrichs, «LCOE: A Useful and Valid Indicator—Replica to James Loewen and Adam Szymanski,» *Energies,* vol. 14, n. 406, 2021.

[38] DNV, “Position Mooring DNV-OS-E301,” DNV, 2008.

[39] SOTRA ANCHOR & CHAIN AS, “Anchor and Chain Handbook,” Norway, 2021.

[40] P. Gómez, G. Sánchez, A. Llana and G. Gonzalez, “COREWIND Deliverable D1.1 Oceanographic and meteorological conditions for the design,” COREWIND, 2015.

[41] B. Steffen, «Estimating the cost of capital for renewable energy projects,» *Energy Economics,* vol. 88, n. https://doi.org/10.1016/j.eneco.2020.104783, 2020.

[42] J. Aldersey-Williams and T. Rubert, “Levelised cost of energy – A theoretical justification and critical assessmen,” *Energy Policy,* no. 124, pp. 169-179, 2019.

[43] IEC, «61400-3 Standard,» IEC, 2019.

[44] F. Papi, Y. Perignon and A. Bianchini, “Derivation of Met-Ocean Conditions for the Simulation of Floating Wind Turbines: a European case study,,” in *Journal of Physics: Conference Series*, 2022.

[45] P. Chaviaropoulos, I. Karga, C. Harkness and B. Hendriks, “PIPI-based Assessment of Innovative Concepts (Methodological Issues),” INNWIND Deliverable 1.2.3, 2014.

[46] M. Ikhennicheu, M. Lynch, S. Doole, F. Borisade, D. Matha, J. L. Dominguez, R. D. Vicente, T. Habekost, L. Ramirez, S. Potestio, C. Molins and P. Trubat, “Review of the state of the art of mooring and anchoring designs, technical COREWIND D2.1,” COREWIND project, 2020.

[47] H. Hersbach, B. Bell, P. Berrisford, S. Hirahara, A. Horányi, J. Muñoz-Sabater, J. Nicolas, C. Peubey, R. Radu, D. Schepers, A. Simmons, C. Soci, S. Abdalla, X. Abellan, G. Balsamo, P. Bechtold, G. Biavati, J. Bidlot and M. Bonavita, “The ERA5 global reanalysis,” *Quarterly Journal of the Royal Meteorological Society,* vol. 146, no. 730, pp. 1999-2495, 2020.

[48] M. R. Patel, Wind and Solar Power Systems, CRC Press, 1999.